Photodisintegration of ^{9}Be with laser-induced Compton backscattered γ rays

H. Utsunomiya, Y. Yonezawa, H. Akimune, T. Yamagata, and M. Ohta
Department of Physics, Konan University, Kobe 658-8501, Japan

M. Fujishiro
Osaka Prefecture University, Sakai 599-8570, Japan

H. Toyokawa and H. Ohgaki
Quantum Radiation Division, Electrotechnical Laboratory, Tsukuba 305-8568, Japan

Photoneutron cross sections were measured for ^{9}Be in the energy range from 1.78 to 6.11 MeV with laser-induced Compton backscattered γ rays. Resonance parameters $[E_R, B(E1), \Gamma_n]$ for the $1/2^+$ and $5/2^+$ states were deduced from the least-squares fit to the data, while Γ_γ for the $5/2^-$ state was deduced from the energy-integrated cross section. The reaction rate $\langle \alpha \alpha n \rangle$ is discussed.

The neutrino-driven wind formed in core-collapse supernovae may be an ideal site for the r process [1]. In this exploding environment, n- and α-rich material is first processed into ^{9}Be through $\alpha(\alpha n, \gamma)^9$Be by bridging mass gaps $A = 5$ and 8 and then ^{9}Be$(\alpha, n)^{12}$C follows. This sequence of ^{12}C production proceeds more efficiently than the triple-α process.

^{9}Be is a loosely bound nuclear system consisting of two α's and a neutron. None of any two constituents can form a bound system. Lifetimes of ^{5}He and ^{8}Be are 1.1×10^{-21} and 0.97×10^{-16} s, respectively. Three adjacent thresholds exist at 1.573 MeV for $\alpha + \alpha + n$, at 1.665 MeV for ^{8}Be$+n$, and at 2.467 MeV for ^{5}He$+\alpha$. In view of the lifetimes, the synthesis of ^{9}Be is considered to proceed more dominantly through ^{8}Be than through ^{5}He. The ternary process is likely to play a minor role. Resonances near threshold govern the rate of the ^{9}Be synthesis. Resonance parameters of these states can be determined by photodisintegrating ^{9}Be.

Previously, photoneutron cross sections near threshold were measured for ^{9}Be using two kinds of real photon sources, Bremsstrahlung and radioactive isotopes. Bremsstrahlung measurements lacked great accuracy due to poor energy resolution [2–4], while radioactive isotope measurements were limited mostly below 2.8 MeV [5–10]. Electron scattering was also used to study low-lying states in ^{9}Be. But the virtual photons excited the $1/2^+$ state only weakly [11,12].

Compton backscattering of laser photons incident on relativistic electrons in the storage ring TERAS of the Electrotechnical Laboratory (ETL) shortens the photon wavelength by a factor of several million, producing quasimonochromatic γ rays [13]. This new MeV photon source is energy variable in the form of a pencil-like beam with a flux of $\sim 10^4$ photons/sec/mm^2 and energy spread of a few percent below 9 MeV [14]. In this Brief Report, we report results of a photoneutron cross section measurement on ^{9}Be in the context of nuclear astrophysics.

Nd:YLF laser photons with $\lambda = 1053$ nm (1.2 eV) were led to a head-on collision point of TERAS. The laser system, which produced 100% linearly polarized light in a normal mode, was operated at 1 kHz. Unpolarized light was also produced by passing through a depolarizer quartz. The laser-induced Compton backscattered (LC) photons were collimated into a spot 2 mm in diameter with a 20 cm thick Pb block at 5.5 m from the head-on collision point. The energy of LC photons was varied by changing the electron energy from 316 to 587 MeV. The energy distribution of LC photons was measured with a pure-Ge detector [efficiency 120% of 3 in.$\times$3 in. NaI(Tl)]. Figure 1 shows a typical spectrum of the LC photons. The full energy peak was calibrated with natural radioactivities ^{40}K and ^{208}Tl as well as a standard ^{60}Co source. Photopeak spectra of the LC photons were previously measured by an anti-Compton spectrometer [14]. They have a characteristic low-energy tail that depends on the divergence and energy spread of the electron beam as well as the collimator size. Because of the low-energy tail, the measurement was limited to $E_\gamma \geq 1.78$ MeV where the photon flux below the neutron threshold (1.665 MeV) can be ignored.

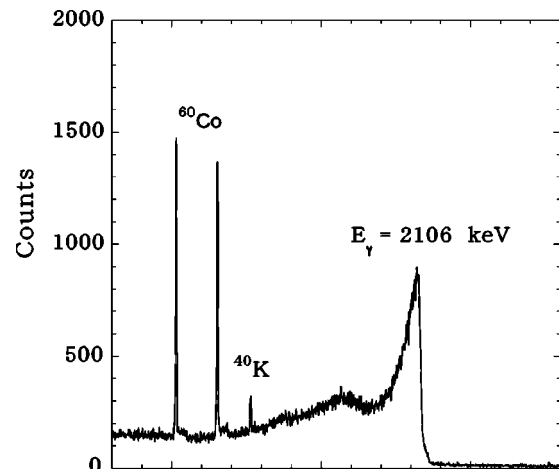A 4 cm thick ^{9}Be rod of 99.5% enrichment (2.5 cm in diameter) was irradiated. Neutrons were measured with four

FIG. 1. A typical energy distribution of LC photons measured with a pure-Ge detector.

63 018801-1

BF$_3$ counters [15] embedded in a 30 cm polyethylene cube. The BF$_3$ counters were located, two each vertically and horizontally, in a concentric ring at 7.5 cm from the beam axis. The distribution of neutron moderation time in the polyethylene was measured. The moderation time constant was found to be 144 μs. Background neutrons that arrived at BF$_3$ counters time independently made a minor contribution to neutron counting.

Neutron detection efficiency was measured at 265 keV with a ^{24}NaOH + D$_2$O source and at the average energy of 2.35 MeV with a ^{252}Cf source. The production of the monoenergetic neutron source and its calibration followed Ref. [10]. Details were reported elsewhere [16]. The energy dependence of the efficiency was calculated with the Monte Carlo code MCNP [17].

LC photons were detected with a BGO detector (2 in. diameter ×6 in. length) placed at the end of the beam line. Pileup spectra were obtained for the 1 kHz LC photons. The average number of photons per beam pulse was determined from the ratio in average channel number between the pileup spectrum and a single photon spectrum. The single photon spectrum was separately taken with a DC beam. The total number of photons were obtained from the frequency and the data acquisition time. Independent test measurements were carried out with a DC beam, in which foreground and background neutrons were measured before and after each measurement with the laser off. Results of the pulsed- and DC-beam measurements agreed with each other to within 5%.

Photoneutron cross sections were obtained from

$$\sigma = \frac{N_n}{N_\gamma \varepsilon_n(E_n) N_t f}, \tag{1}$$

where N_n is the number of neutrons detected, N_γ is the number of LC photons incident on the BGO detector, N_t is the number of target nuclei per cm^2, and $\varepsilon_n(E_n)$ is the neutron detection efficiency. A correction factor, f, was needed for a thick target measurement:

$$f = e^{\mu t} \frac{(1 - e^{-\mu t})}{\mu t}. \tag{2}$$

μ is the total γ-attenuation coefficient in ^{9}Be [18] and t is the length (4 cm) of the target material.

Photoneutron cross sections measured with polarized and unpolarized photons are shown by solid and open circles in Fig. 2, respectively. The decay channel was assumed to be $n + ^8$Be. Horizontal error bars stand for the skewed energy spread of LC photons in FWHM. As for vertical error bars, only statistical uncertainties are shown. The results of polarized and unpolarized photon measurements at 1.9, 2.7, and 3.3 MeV agreed with each other within statistics. The lineshape of broad resonance states was determined by the present measurement, whereas that of the narrow state at 2.44 MeV with a width less than 1 keV [19] was not determined. The cross section for the 2.44 MeV state showed a sudden rise due to the photopeak edge of the LC photons followed by a gradual decrease due to the low-energy tail of the LC photons.
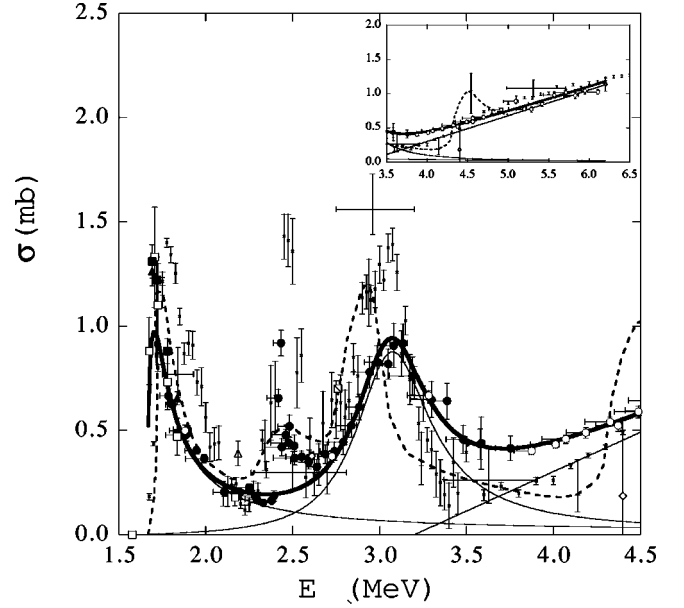

FIG. 2. Photoneutron cross sections for ^{9}Be (solid circles for polarized LC photons and open circles for unpolarized LC photons). Data taken with bremsstrahlung (dotted line [2], large crosses [3], and crosses [4]) and radioactive isotopes (open squares [10], solid squares [9], solid triangles [8], open triangle [6], slashed-open square [5], and diamonds [7]) are also shown. The best least-squares fit is shown by the solid lines (thick solid line for sum and thin solid lines for breakdown).

The effect of asymmetric photoneutron emission on $\varepsilon_n(E_n)$ was investigated with help of the MCNP code. For the asymmetries $a/b = 1.2$ [20] and 1.0 [2] in $a + b \sin^2\theta$ reported at 2.76 and 2.95 MeV, respectively, the associated uncertainty was found to be 9–12 %. This is regarded as the systematic uncertainty in the present measurement.

For comparison, cross sections measured with other photon sources are also shown in Fig. 2. The horizontal error bars of the large crosses [3] as well as the dotted bump [2] corresponding to the 2.44 MeV state ($\Gamma < 1$ keV) represent the energy resolution of bremsstrahlung measurements. The three bremsstrahlung measurements do not give consistent results for the 1.7 MeV and 3 MeV states both in energy and magnitude [2–4]. The result of the radioactive-isotope measurement for the 1.7 MeV state [10] is consistent with the present result.

The least-squares fit to the data was performed with the cross section of Breit-Wigner form:

$$\sigma_{\gamma,n}(E_\gamma : I \rightarrow J) = \pi \frac{2J+1}{2(2I+1)} \left(\frac{\hbar c}{E_\gamma}\right)^2 \frac{\Gamma_\gamma \Gamma_n}{(E_\gamma - E_R)^2 + (\Gamma/2)^2}. \tag{3}$$

γ-decay widths for $E1$ and $M1$ are expressed [21], respectively, by

$$\Gamma_\gamma(E1) = \frac{16\pi}{9} \alpha(\hbar c)^{-2} E_\gamma^3 B(E1) \tag{4}$$

and

TABLE I. Comparison of the present work with results of (e,e') scattering experiments.

I^π	$X\lambda$	E_R (MeV)		$B(E1\downarrow)$ (e^2 fm^2)		$\Gamma \simeq \Gamma_n$ (keV)	
		(e,e')	Present (γ,n)	(e,e')	Present (γ,n)	(e,e')	Present (γ,n)
$1/2^+$	$E1$	1.78 ± 0.03[a]	1.748 ± 0.01	0.050 ± 0.020[a]	0.107 ± 0.007		283 ± 42
		1.684 ± 0.007[b]		0.054 ± 0.004[b]		217 ± 10[b]	
$5/2^-$	$M1$	2.44 ± 0.02[a]	2.43	0.089 ± 0.010[a,c]	0.049 ± 0.012 [c]		
$5/2^+$	$E1$	3.04 ± 0.03[a]	3.082 ± 0.012	0.010 ± 0.008[a]	0.039 ± 0.002		533 ± 19

[a]Reference [11].
[b]Reference [12].
[c]Γ_γ in eV.

$$\Gamma_\gamma(M1) = \frac{16\pi}{9}\alpha(2Mc^2)^{-2}E_\gamma^3 B(M1), \quad (5)$$

where α is the fine-structure constant, M is the proton mass, and $B(E1)$ and $B(M1)$ are reduced transition probabilities given in units of e^2 fm^2 and $(e\hbar/2Mc)^2$. Γ_n for s-wave neutrons from $1/2^+$ was taken [22] as

$$\Gamma_n = 2\sqrt{\epsilon_R(E_\gamma - E_T)}. \quad (6)$$

This form of neutron decay width leads to single-level approximation of R-matrix theory [23]. Γ_n for other states was taken to be energy-independent.

We used the energy-integrated cross section [24] to deduce Γ_γ for the narrow resonance state at 2.44 MeV:

$$\int_0^\infty \sigma_{\gamma,n} dE_\gamma = \frac{3\pi^2}{2}\left(\frac{\hbar c}{E_R}\right)^2 \Gamma_\gamma. \quad (7)$$

The least-squares fit was performed to 49 data points up to 4.5 MeV. The 49 data points did not include the data for the 2.44 MeV state, but did include those of Fujishiro *et al.* [10]. The $E1$ and $M1$ parametrizations were employed for the positive- and negative-parity states $(1/2^+, 5/2^+, 1/2^-)$, respectively. A straight-line background $(\sigma = 0.38E_\gamma - 1.21$ mb) was assumed in the high-energy region. The least-squares fit resulted in the χ^2 minimum with $B(M1)=0$ for $1/2^-$. Thus, the presence of $1/2^-$ was not confirmed as was the case in the electron scattering. The best fit $(\chi^2 = 2.7$ per degree of freedom) is shown by the thick solid line in Fig. 2.

The best-fit parameters along with 1 σ uncertainties from the error matrix are listed in Table I. For comparison, the results of (e,e') scattering are also listed. The $B(E1\downarrow)$ value for $1/2^+$ is approximately twice those of [11,12], while it is close to that $(0.106^{+0.019}_{-0.016})$ deduced from R-matrix fit to Fujishiro data alone [25]. Γ_γ for $5/2^-$ is roughly half the (e,e') value. $B(E1\downarrow)$ for $5/2^+$ is four times the (e,e') value. It was pointed out [25] that the discrepancy for $1/2^+$ between the (γ,n) [10] and the (e,e') [11] results may be due to background subtraction in the electron scattering. It was shown that good agreement between the two was obtained by integrating the (γ,n) cross section up to 2 MeV [25].

Woosley and Hoffman used the rate $\langle\alpha\alpha n\rangle$ of the Caughlan and Fowler compilation [26] for the nucleosynthesis calculation in core-collapse supernovae [1]. This reaction rate has been updated in the 1999 compilation [27] which relied on three resonances, neglecting $5/2^-$. It employed $\Gamma_\gamma = 0.51 \pm 0.10$ eV for $1/2^+$ from (γ,n) [10], $\Gamma_\gamma = 0.90 \pm 0.45$ eV for $5/2^+$ from (e,e') [3] with an increased error, and assumed $\Gamma_\gamma = 1$ W.u. for $1/2^-$ with 80% error.

We evaluated the rate $\langle\alpha\alpha n\rangle$ based on the resonant contribution to the reaction $\alpha + \alpha \rightleftharpoons {}^8$Be with $\Gamma_\alpha({}^8$Be$) = 6.8 \pm 1.7$ eV. This resonant condition is known to hold at $T > 2.8 \times 10^7$ K [28].

The rate $\langle n^8\text{Be}\rangle$ is calculated from

$$\langle n^8\text{Be}\rangle = N_A\left(\frac{8}{\mu\pi}\right)^{1/2}(kT)^{-3/2}\int_0^\infty \sigma^{capt}(E)E$$
$$\times \exp\left(-\frac{E}{kT}\right)dE. \quad (8)$$

The best fit cross section of Breit-Wigner form was converted by the detailed balance theorem to radiative capture cross sections (σ^{capt}) for $n + {}^8\text{Be} \rightarrow {}^9\text{Be} + \gamma$. As for $5/2^-$, the present Γ_γ was used together with $E_R = 2429$ keV and $\Gamma = 0.77 \pm 0.15$ keV [19]. The ratio of the result to the rate in the 1999 compilation is shown by the thick solid line in Fig.
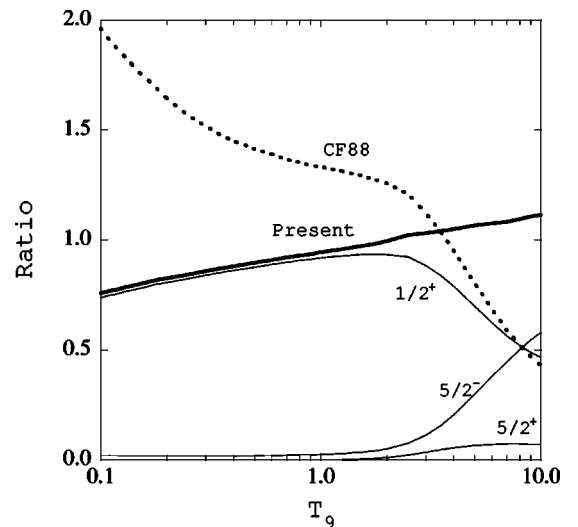

FIG. 3. Ratio of the present $\langle\alpha\alpha n\rangle$ to the rate of the 1999 compilation [27] (thick solid line for sum and thin solid lines for breakdown). The ratio of the Caughlan and Fowler 1988 rate [26] to that of the compilation is also shown by the dotted line.

3. The deviation ranges from -25% to $+11\%$ at $T_9 \geqslant 0.1$. The relatively small deviation is because of the Γ_γ employed for the leading $1/2^+$ state in the compilation. The breakdown of the rate into contributions from each states is also shown by thin solid lines. The contribution of $5/2^-$ become important at $T_9 > 1.0$, while the $5/2^+$ state marginally contributes even at high temperatures. Since the rate in [27] neglected the $5/2^-$ contribution, it is most likely that the strength (1 W.u.) taken *a priori* for $1/2^-$ compensated the rate.

In summary, the LC photon source was used to measure photoneutron cross sections for ^{9}Be (Fig. 2). Resonance parameters for $1/2^+$, $5/2^-$ and $5/2^+$ states were deduced from the least-squares fit as well as the integrated Breit-Wigner form (Table I). In the context of nuclear astrophysics, it was found that the rate of the 1999 compilation [27] is consistent with the present evaluation within 36% at $T_9 \geqslant 0.1$ (Fig. 3), while the Caughlan and Fowler rate needs a considerable modification in both T_9 dependence and magnitude to within a factor of ± 2 over the temperature range.

[1] S.E. Woosley and R.D. Hoffman, Astrophys. J. **395**, 202 (1992).
[2] M.K. Jakobson, Phys. Rev. **123**, 229 (1961).
[3] R.J. Hughes *et al.*, Nucl. Phys. **A238**, 189 (1975).
[4] A.M. Goryachev, G.N. Zalesny, and I.V. Pozdnev, Izv. Ross. Akad. Nauk, Ser. Fiz. **56**, 159 (1992).
[5] B. Russel *et al.*, Phys. Rev. **73**, 545 (1948).
[6] B. Hamermesh and C. Kimball, Phys. Rev. **90**, 1063 (1953).
[7] R.D. Edge, Nucl. Phys. **2**, 485 (1956/57).
[8] J.H. Gibbons *et al.*, Phys. Rev. **114**, 1319 (1959).
[9] W. John and J.M. Prosser, Phys. Rev. **163**, 958 (1967).
[10] M. Fujishiro *et al.*, Can. J. Phys. **60**, 1672 (1982); **61**, 1579 (1983).
[11] H.-G. Clerc *et al.*, Nucl. Phys. **A120**, 441 (1968).
[12] G. Kuechler *et al.*, Z. Phys. A **326**, 447 (1987).
[13] H. Toyokawa *et al.*, Nucl. Instrum. Methods Phys. Res. A **422**, 95 (1999).
[14] H. Ohgaki *et al.*, IEEE Trans. Nucl. Sci. **38**, 386 (1991).
[15] MITSUBISHI ND8534-60 BF$_3$ counters with the dimension 2.5 cm in diameter $\times$24.1 cm in effective length and the gas pressure 600 torr.
[16] Y. Yonezawa and H. Utsunomiya, Mem. Konan Univ., Sci. Ser. **46**, 43 (1999).
[17] J.F. Briesmeister, MCNP, A General Monte Carlo N-Particle Transport Code, Version 4B, Las Alamos National Laboratory, 1997.
[18] *Engineering Compendium on Radiation Shielding, Vol. 1*, edited by R.G. Jaeger, E.P. Blizard, A.B. Chilton, M. Grotenhuis, A. Hönig, Th. A. Jaeger, and H.H. Eisenlohr (Springer-Verlag, New York, 1968), p. 173.
[19] F. Ajzenberg-Selove, Nucl. Phys. **A413**, 1 (1984).
[20] B. Hamermesh *et al.*, Phys. Rev. **76**, 611 (1953).
[21] J.M. Blatt and V.F. Weisskopf, *Theoretical Nuclear Physics* (Springer-Verlag, New York, 1952), p. 583.
[22] F.C. Barker and B.M. Fitzpatrick, Aust. J. Phys. **21**, 415 (1968).
[23] A.M. Lane and R.G. Thomas, Rev. Mod. Phys. **30**, 257 (1958).
[24] F.C. Barker, Nucl. Phys. **28**, 96 (1961).
[25] F.C. Barker, Can. J. Phys. **61**, 1371 (1983).
[26] G.R. Caughlan and W.A. Fowler, At. Data Nucl. Data Tables **40**, 283 (1988).
[27] C. Angulo *et al.*, Nucl. Phys. **A656**, 3 (1999).
[28] K. Nomoto, F.-K. Thielemann, and S. Miyaji, Astron. Astrophys. **149**, 239 (1985).